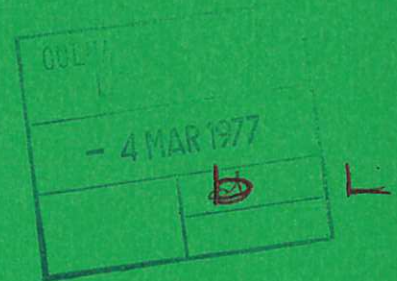


This document is intended for publication in a journal, and is made available on the understanding that extracts or references will not be published prior to publication of the original, without the consent of the authors.

CLM - P 462



UKAEA RESEARCH GROUP

Preprint

SUB-NANOSECOND RISETIME LASER PULSE GENERATION WITH A FAST DIELECTRIC SWITCH AND POCKELS CELL

P D WILCOCK
B C FAWCETT
G E BROMAGE

CULHAM LABORATORY
Abingdon Oxfordshire

1977

This document is intended for publication in a journal or at a conference and is made available on the understanding that extracts or references will not be published prior to publication of the original, without the consent of the authors.

Enquiries about copyright and reproduction should be addressed to the Librarian, UKAEA, Culham Laboratory, Abingdon, Oxfordshire, England

MEASUREMENTS

Records taken with 2 ns and 4 ns duration pulses applied to the Pockels cell are chosen to illustrate the risetime (see Figs.3a,b,c,d). Figs.3a and 3b show the 4 ns optical pulse-width records on a slow timescale as a photograph and tracing. Because of the faintness of the photographic records on a fast oscilloscope scan, tracings only are shown (Figs.3c and 3d) for 4 and 2 ns pulses. Other pulse lengths were achieved by changing the length of the Blumlein. In each case the risetime was as illustrated, rising from 10% to 90% of the maximum measured on the oscilloscope scale in $1.1 \text{ ns} \pm 10\%$. The oscilloscope time calibration was checked. Of the 1.1 ns, contributions to the measurement came from the 350 ps oscilloscope risetime and from the 200 ps photodiode risetime. A simple analysis of the degradation of the real pulse by these risetimes with an analogue computer yields the real optical risetime of 990 ps (see appendix). This results from the combined effect of the spark gap, Pockels cell and cable junctions. From electrical measurements made separately with fast pick-up monitors in the braid of the coaxial cable joined to the Pockels cell and spark gap, it was found that each contributed less than 400 ps to the sub-nanosecond risetime, with the remainder added by cable junctions. Fig.4 shows an oscilloscope trace of the diode output, while measuring light reflected from inside the oscillator cavity, superimposed on light switched out by the Steinmetz cell. It indicates that the output light pulse occurs at the time of peak build-up of radiation in the oscillator cavity. The 33 ns delay, shown in Fig.4, between the start of the 40 ns pulse and the PTM pulse, can be reduced either by decreasing the thickness of the melinex or increasing the light intensity per unit area focused on its surface. This was verified by experiment.

DISCUSSION

The advantages of the DSG and the quarter-wave switching technique used in this project can be summarised as follows:

- a. The present models of switch maintained their performance over a range of 1 kV to 25 kV, whereas gas-filled spark gaps deteriorate in jitter and risetime below 7 kV, as shown by Bettis and Guenther (1970).
- b. Two of the four switch outputs remain free to operate another synchronised Pockels cell (minor redesign of the DSG can provide extra outputs).
- c. Risetime and pulse length are independent parameters, but they are not independent for pulse-clipping modes of operation in which transmission through the Pockels cell and associated polariser occurs only during the rising edge of the pulse (such as reported by Morgan and Peacock (1971) for nanosecond pulse durations).

d. For multi-shot operation a dielectric tape can be fed through the space between the electrodes by a mechanical device. In the present low current application there is negligible electrode wear so that replacement of the gap will rarely be necessary.

For other projects which require much shorter light-pulse risetimes a reduction in risetime can be obtained by several means:

Firstly, the adoption of a lower design voltage for the switch and Pockels cell will allow a reduction in dimensions and hence in the inductances and capacitances on which risetime depends. Secondly, the replacement of the two 50 Ω output cables by four of 100 Ω would approximately halve the L/R time of the switch, whilst maintaining impedance-matching to the Steinmetz cell. Thirdly, the use of the DSG and Steinmetz cell in the pulse-clipping system referred to above would shorten pulse risetimes.

ACKNOWLEDGMENTS

The contribution from the Appleton Laboratory is published with the permission of the Director. The authors thank K. Sinton for performing calculations with an analogue computer.

REFERENCES

- Alcock, A.J. Richardson, M.C. Leopold, K. 1970. Rev.Sci. Instrum. 41. 1028-9.
- Bettis, J.R. Guenther, A.H. 1970. Quantum Electron. QE6. 483-91.
- Dewhurst, R.J. Pert, G.J. Ramsden, S.A. 1972, J. Phys. D. Appl. Phys. 5, 97-103.
- Ireland, C.L.M. 1975, J. Phys. E. 8, 1007-10.
- Michon, M. Guillet, H. Gaff, D. Reynaud, S. 1969, Rev. Sci. Instrum, 40, 263-5.
- Morgan, P.D. Peacock, N.J. 1971, J. Phys.E. Scientific Instruments, 4, 677-80.
- Steinmetz, L.L. Pouliot, T.W. Johnson, B.C. 1973, Appl. Opt. 12, 1468-71.

APPENDIX

A simple analysis has been performed using an analogue computer to evaluate the degree to which input waveshapes had been degraded in the measured waveforms by the circuit time constants.

The assumptions made were that the waveshapes were exponential and that measured and quoted risetimes were 10% to 90% figures. From a waveform generation point of view the exponential shape is likely to be a good assumption, since exponential rises of voltage with time constants related to L/R or RC can usually be shown to dominate. Through cascaded time constants the assumption is less accurate. From the two assumptions it can be shown that the measured risetime (10%-90%) is 2.2 times the exponential time constant. Specification risetimes of the oscilloscopes used were quoted 10%-90% in the same manner and the same factor was used.

The following cases were investigated.

1. The measured voltage risetime at the cable end remote from the switch was calculated. Four modifying time-constants were identified.
 - a. That produced by inductance of the connection loop to the voltage divider with the divider resistance (L/R).
 - b. That produced by the divider resistance with the stray capacitance (CR).
 - c. The effective figure from the frequency response characteristic of the signal cable.
 - d. The risetime specification of the measuring oscilloscope.

Considering these in order, (a) the connection loop size was calculated to give approximately 40 nH, giving, with the divider resistance, an L/R time constant of 150 ps. No calculations or estimates were made on item (b) so no allowance for degradation from this cause was included. No precise measurements were made of item (c) but previous measurements of the degradation of fast pulse fronts as the length of the cable was varied, suggest that the contribution from this source, with the short length of measuring cable used, could be ignored. The time-constant associated with oscilloscopes used was calculated from the specification to be 160 ps.

The analogue computer was used to evaluate the exponential input voltage risetime that would give the measured response of 10%-90% in 600 ps after two stages of 160 ps time-constant. The result is shown in Fig.5.

2. The other case evaluated was the optical output pulse measuring circuits, where

**SUB-NANOSECOND RISETIME LASER PULSE GENERATION
WITH A FAST DIELECTRIC SWITCH POCKELS CELL**

Wilcock, P. D.

Culham Laboratory, Abingdon, Oxon, OX14 3DB, United Kingdom

Euratom-UKAEA Fusion Association

Fawcett, B. C. Bromage, G. E.

Appleton Laboratory, Astrophysics Research Division,
Science Research Council, Culham Laboratory, Abingdon, Oxon.

ABSTRACT

A new solid-dielectric laser-triggered spark gap operated in conjunction with a cylindrical-electrode Pockels cell has achieved sub-nanosecond optical risetimes for shuttered laser pulses using quarter-wave switching. Switching in this mode has the advantage that risetime and pulse length are independent parameters. The gap offers an advantage over gas-filled laser-triggered spark gaps for switching voltages near 4 kV and can operate synchronised Pockels cells.

(Submitted for publication in Journal of Physics E)

INTRODUCTION

A new solid-dielectric laser-triggered spark gap (DSG) has been operated as a sub-nanosecond switch for a Pockels cell acting as a light shutter in a giant pulse Q-switched laser. When used in conjunction with an ultra-fast risetime cylindrical-electrode Pockels cell (Steinmetz et al. 1973) supplied by Electro Optic Developments (Type PC 105), sub-nanosecond risetimes were measured for the shuttered optical pulse. The new ultra-fast Steinmetz-type Pockels cells operate at lower voltages than conventional ring-electrode Pockels cells. In this lower voltage regime the DSG is superior to gas-filled laser-triggered spark gaps (GSG) (Ireland, 1975) in that the risetime and jitter of the GSG deteriorates with decreasing voltage below 7 kV. The purpose of the present development is to provide new elegant solution to a difficult switching problem; a solution which may be preferable in some circumstances partly because of the fundamental importance of this extension of the range of ultra-fast switching to lower voltages with the added bonus of the ability to use the same switch over an extended voltage range. Other GSG are reported by Michon et al. (1969), Alcock et al. (1970), Bettis and Guenther (1970) and Dewhurst et al. (1972). As in the case of the multichannel GSG of Ireland (1975) the DSG can meet the requirements of some Q-switched lasers for sub-nanosecond synchronised switching of more than one Pockels cell. By connecting the Pockels cell to the DSG via Blumleins of different lengths, the duration of light pulses switched directly out of the laser oscillator cavity could be varied from 1 ns upwards.

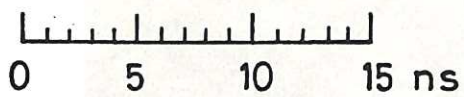
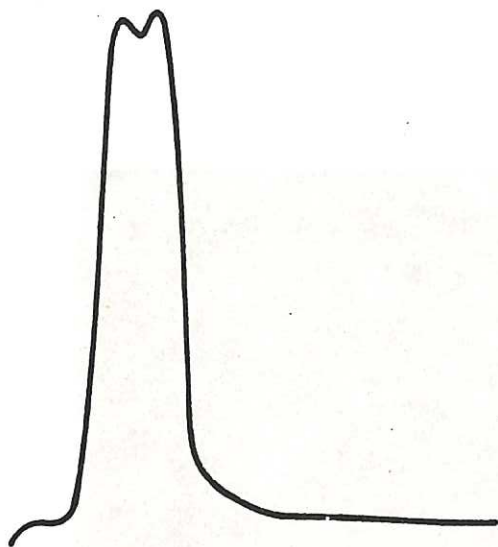
DESCRIPTION OF APPARATUS

Figure 1 shows a cross section of the DSG. As with the GSG of Ireland (1975) the coaxial cables are arranged symmetrically around the spark. There are four output cables situated at four out of six equi-spaced points on a circle 41 mm in diameter. The solid dielectric spark-gap was designed to provide the best possible short circuit (lowest switch inductance and resistance) to the four output cables when the spark gap was triggered, consistent with safety from spurious breakdown at the design maximum voltage of 20 kV. The voltage grading at the electrode surfaces and cable entries minimises tangential electric stress at the insulation junctions and reduces the clearances that are necessary to resist surface tracking, and hence the inductance is kept to a minimum. The electrodes each have silicone

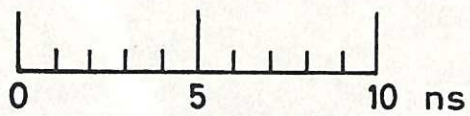
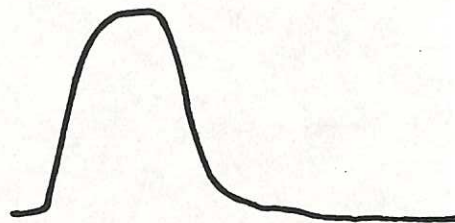
rubber moulded insulation and plane contact surfaces. The insulation distorts sufficiently to maintain intimate contact when the thin melinex gap insulation is sandwiched between the faces under the mount pressure. The uniformity of the electric stress permits the melinex to be used at higher voltage stress than usual and thus thinner insulating films can withstand the design voltage without tracking or puncture. The resultant very small electrode separation gives reliable, low-jitter triggering over the range 3-20 kV, producing a short arc length which aids the low inductance and resistance requirements of the switch. The capacitance of the switch is also too small to have any appreciable effect on the pulse rise-time. When 75 μm melinex was used as the solid dielectric, the switch held off 25 kV. With this, a voltage risetime of 600 picoseconds was recorded on a clean square-topped pulse from four 50 Ω cables in parallel; this risetime is the real risetime degraded by the oscilloscope (Tektronix 519 of nominal risetime 350 ps) and the voltage divider (a locally-manufactured, fast-response design with connection risetime, associated with L/R, of 350 ps). Simple analysis by analogue computer (see appendix) yields a real 10% to 90% risetime for the switch of 290 ps.

In the optical measurements reported here two 50 Ω cables (Uniradio 67) were connected into two diametrically opposite spark-gap connections. These were used as switching leads for two parallel Blumlein transmission lines. The Blumlein outputs were joined to a 50 Ω coaxial cable which delivered the output pulse to a Steinmetz-type Pockels cell (see Fig.2a). The cell was impedance-matched to 50 Ω and had input and output terminals which were connected to the 50 Ω line and a 50 Ω cylindrical carbon low-inductance resistor, respectively. The Blumlein therefore delivered a square voltage output pulse to the Pockels cell which was dumped in the 50 Ω resistor.

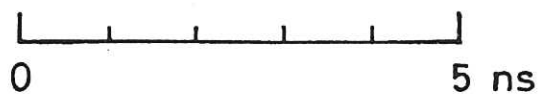
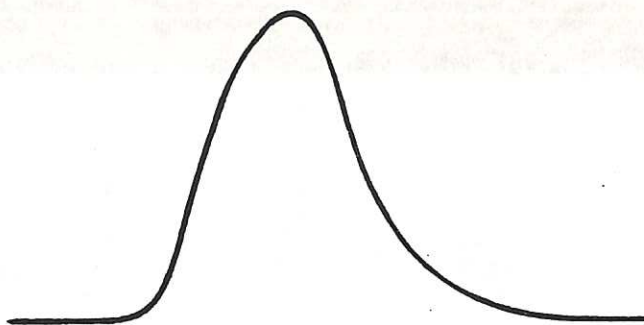
Components of the neodymium laser oscillator were arranged in the following order (Fig.2b): 80% reflecting dielectric end mirror, Steinmetz-type Pockels cell, Glan-Taylor polariser, neodymium rod, stack polariser, conventional Pockels cell, and totally reflecting dielectric end mirror. The oscillator was operated in the pulse transmission mode. Quarter-wave switching of the conventional Pockels cell provided a 40 ns half-width laser output pulse through the 80% reflecting mirror. This was focused to trigger the spark gap with the Blumlein charged to 3.5 kV. A 3.5 kV square pulse consequently arrived at the Steinmetz Pockels cell and switched it to a quarter wavelength for neodymium radiation. A square light pulse was therefore reflected out of the laser cavity by the Glan-Taylor polariser. A fraction of this output was monitored with a 200 ps time-response Instrument Technology photodiode, and its output current recorded by a Tektronix 519 oscilloscope (350 ps time response) and camera.



3b 4 ns (FWHM) pulse: tracing of a 10 ns/cm scan.



3c 4 ns (FWHM) pulse: tracing of a 5 ns/cm scan.



3d 2 ns (FWHM) pulse: tracing of a 5 ns/cm scan.

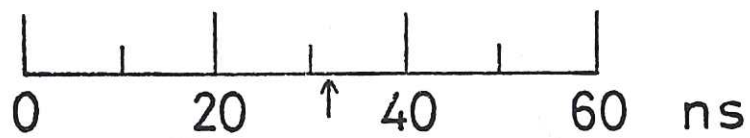
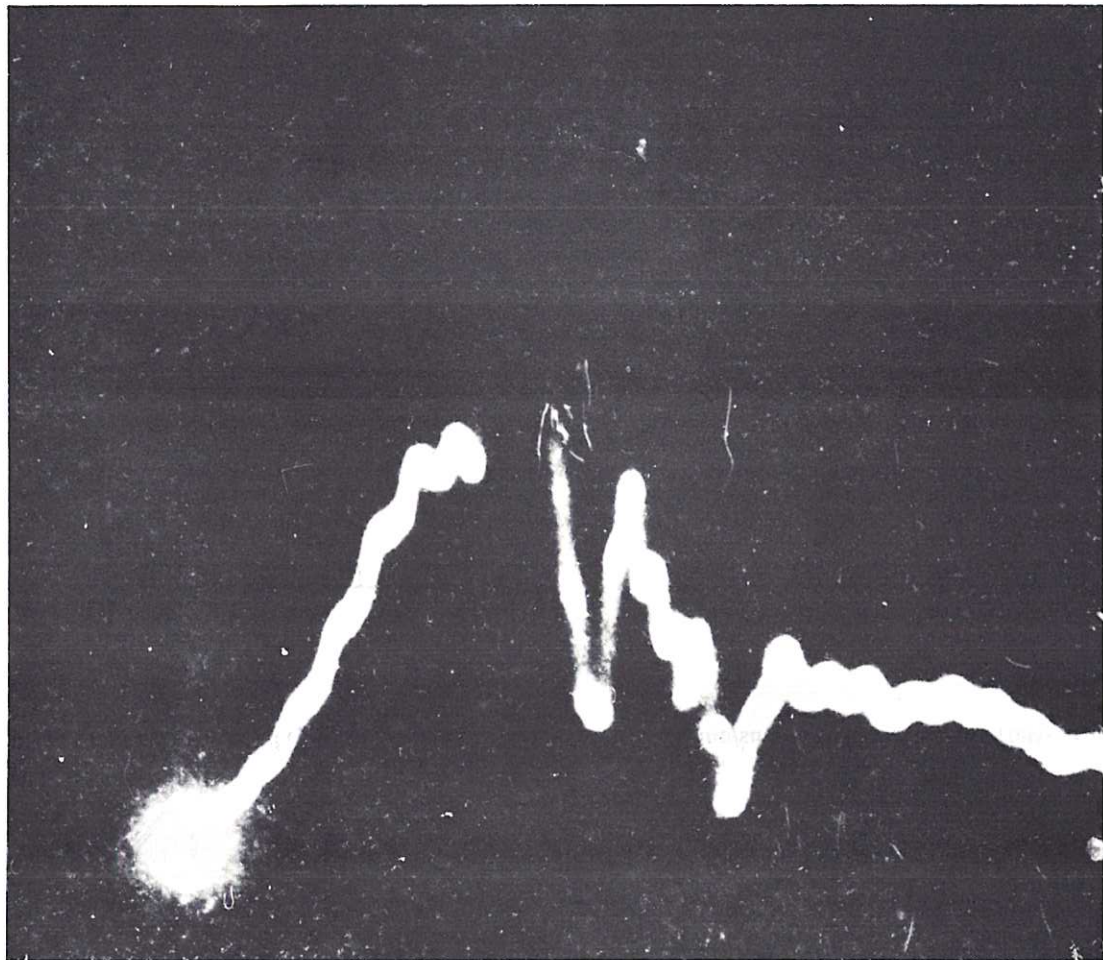


Fig.4 Oscilloscope record of photodiode signal for a switched-out pulse (as in Fig.3), sampled together with a small fraction of the main laser pulse within the cavity, and recorded simultaneously. The arrow indicates the time at 10% of peak intensity of the switched-out pulse: in this example, this occurs 33 ns after the start of the main pulse and at its maximum intensity.

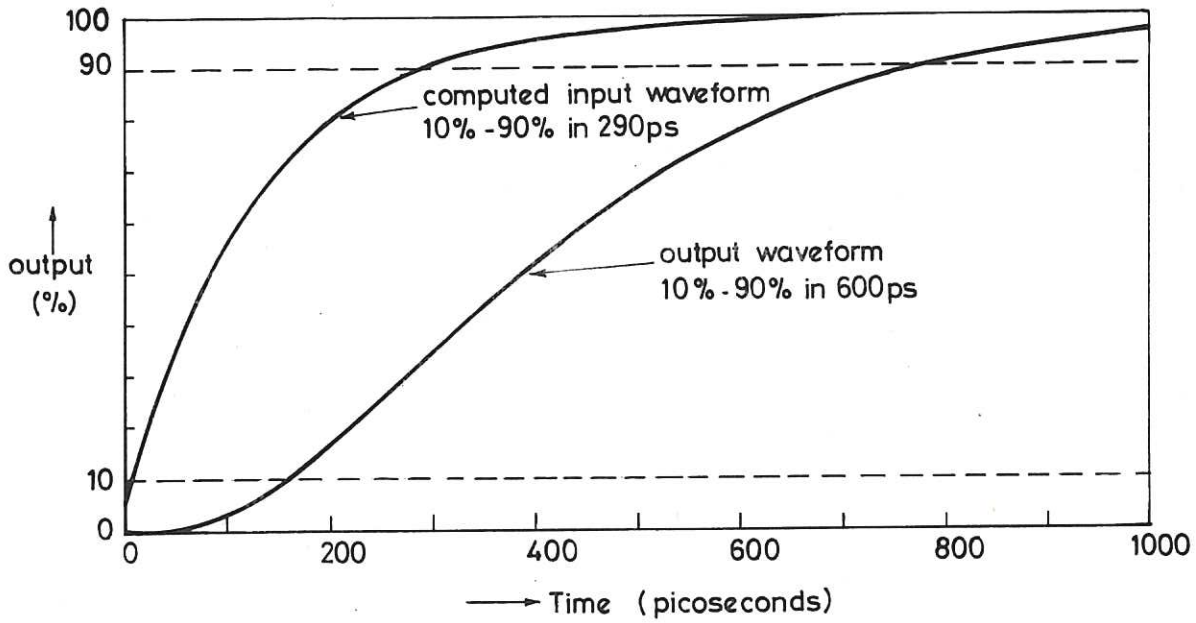


Fig.5 Simulated electrical waveforms (Appendix, case 1) for measured output risetime (10% to 90%) of 600ps and two degrading contributions with exponential time-constants of 160ps each.

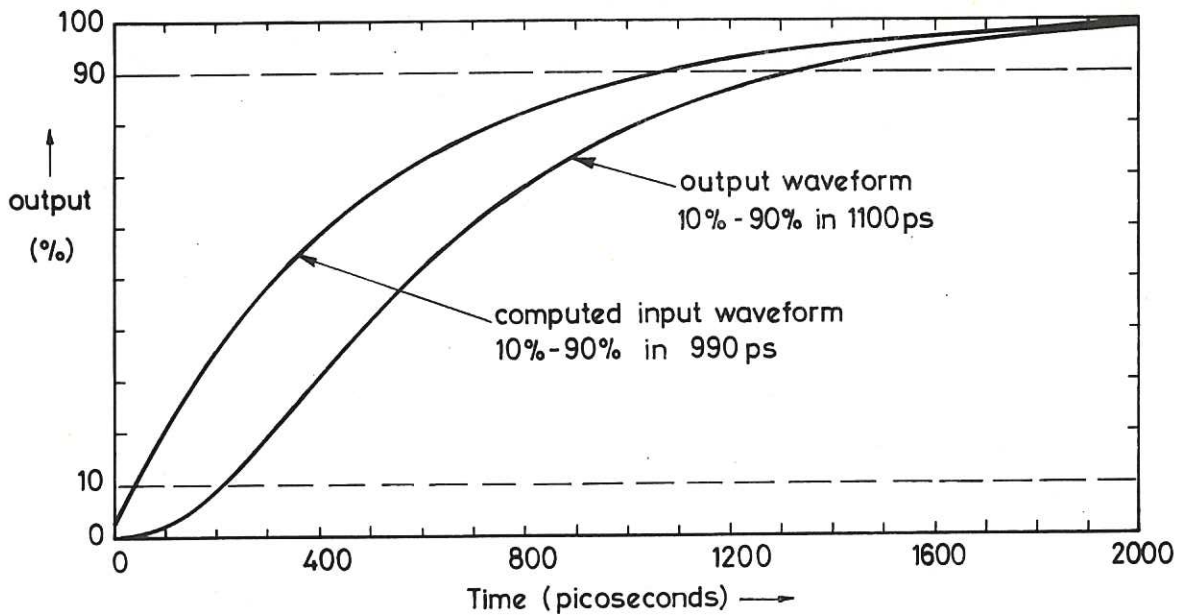


Fig.6 Simulated optical waveforms (Appendix, case 2) for measured output risetime (10% to 90%) of 1100ps and two degrading contributions with exponential time-constants of 90ps and 160ps respectively.

three modifying time-constants are involved.

- a. The measuring photodiode - specification risetime 200 ps (assumed as 10%-90%, given exponential time-constant of 91 ps).
- b. The signal cable - where the same statements as before apply.
- c. The measuring oscilloscope - 160 ps as before. The results of this analysis are shown in Fig.6.

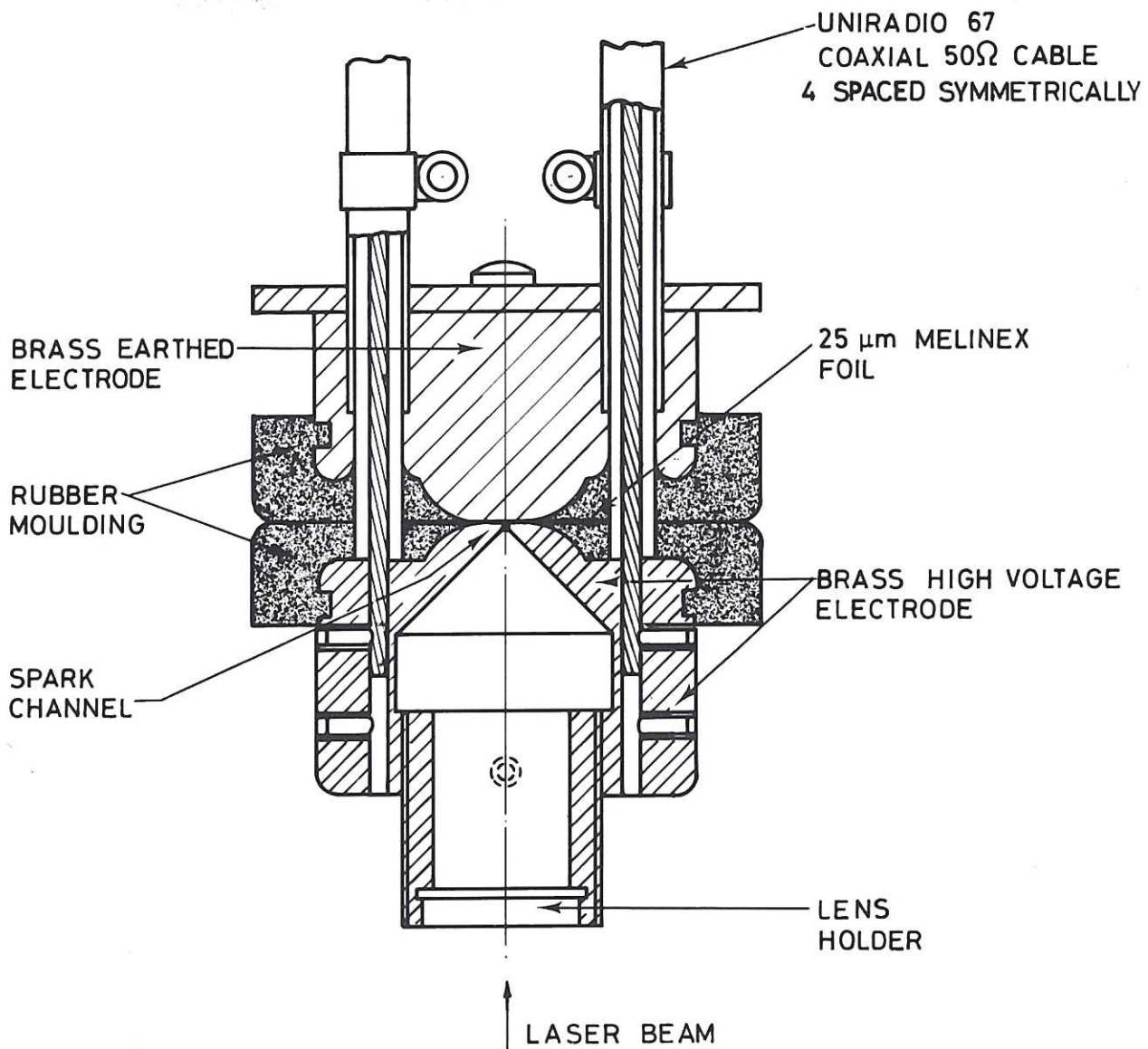


Fig.1 Cross-section of the solid-dielectric laser-triggered spark gap assembly.

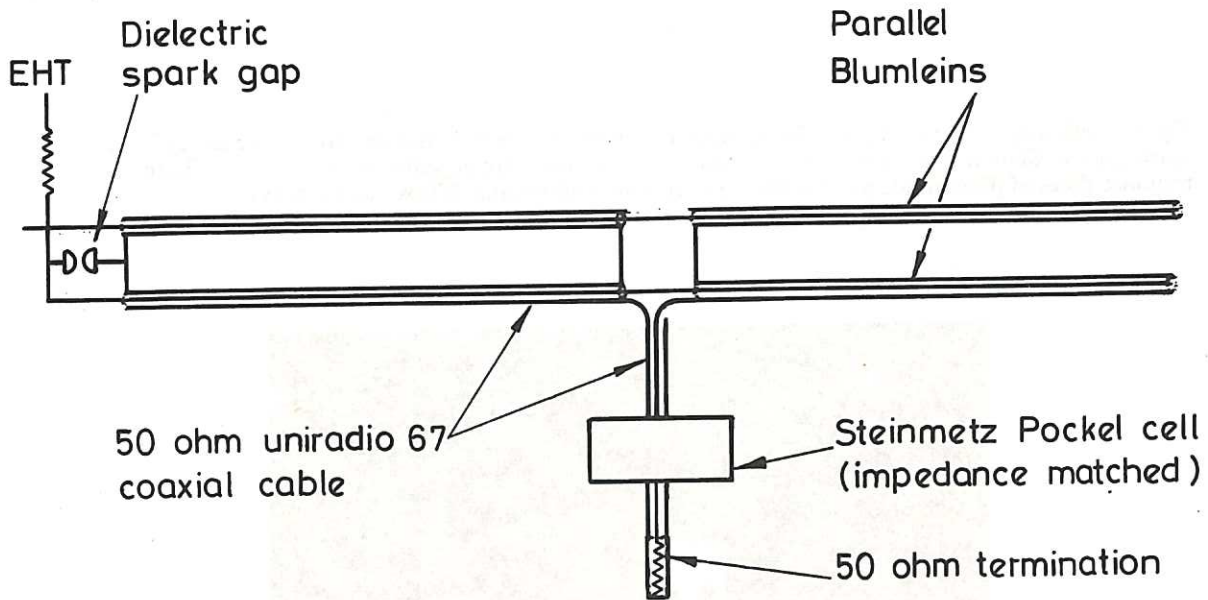
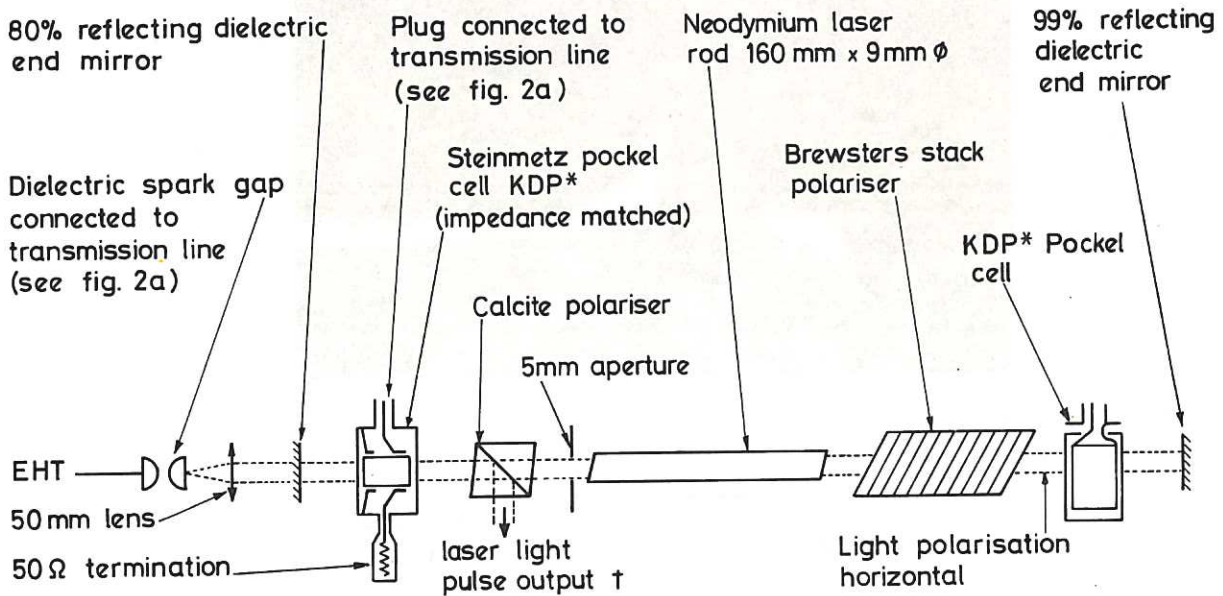


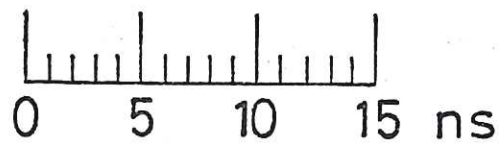
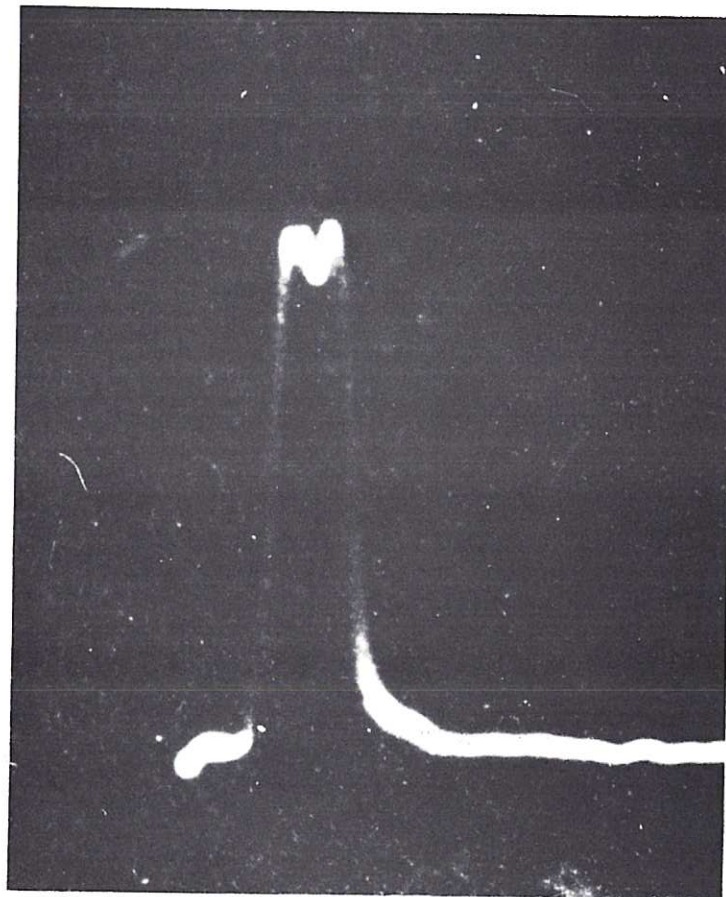
Fig.2a Schematic diagram of the switching circuit.



- † Laser light pulse output is vertically polarised
- † Pulse durations : -
- a) Laser light pulse output adjustable from 1 to 10 ns
- b) Inside cavity 40 ns

Fig.2b Schematic diagram of the neodymium glass laser oscillator, incorporating spark gap and Steinmetz Pockels cell.

Fig.3 Oscilloscope records of photodiode signal for optical pulses switched out from laser cavity by the spark gap and Steinmetz Pockels cell. The observed waveforms are degraded by the inherent finite response times of photodiode and oscilloscope (risetimes 200 ps and 350 ps, respectively).



3a 4 ns (FWHM) pulse: photograph of a 10 ns/cm scan.

The first part of the document discusses the importance of maintaining accurate records of all transactions. It emphasizes that every entry, no matter how small, should be recorded to ensure the integrity of the financial statements. This includes not only sales and purchases but also expenses and income. The document provides a detailed explanation of how to categorize these transactions and how to use a double-entry system to ensure that the books are balanced.

Next, the document covers the process of reconciling bank statements. It explains that this is a crucial step in verifying the accuracy of the cash account. The process involves comparing the bank's records with the company's records and identifying any discrepancies. Common reasons for discrepancies include bank charges, interest, and timing differences. The document provides a step-by-step guide to performing a bank reconciliation and includes a sample reconciliation form.

The third section discusses the preparation of financial statements. It outlines the steps involved in calculating the net income, preparing the balance sheet, and the income statement. The document emphasizes the importance of accuracy and transparency in these statements, as they provide a clear picture of the company's financial performance. It also discusses the importance of comparing these statements to the previous period to identify trends and areas for improvement.

Finally, the document provides a summary of the key points discussed and offers some final thoughts on the importance of good financial management. It encourages the reader to take the time to understand the basics of bookkeeping and to apply these principles in their own business. The document concludes with a list of resources for further learning and a contact information for the author.

